LASER ASSISTED SEPARATION PROCESSES FOR BIFACIAL *p*SPEER SHINGLE SOLAR CELLS

A. Münzer, P. Baliozian, K. Ahmed, A. Nair, E. Lohmüller, T. Fellmeth, A. Spribille, R. Preu
Fraunhofer Institute for Solar Energy Systems ISE, Heidenhofstraße 2, 79110 Freiburg, Germany

ABSTRACT: In this paper, two laser-assisted separation processes (i) laser scribe and mechanical cleaving (LSMC) and (ii) thermal laser separation (TLS) for the separation of *p*-type silicon shingled passivated edge, emitter and rear (*p*SPEER) solar cells are examined. Both separation processes involve two process steps, where one of them is considered the main laser process that is conducted along the whole separation path (laser scribe for LSMC and laser cleave for TLS). We analyze the influence of the main laser process as well as the complete separation process of both, LSMC and TLS, on the electrical performance of *p*SPEER solar cells. We include an investigation of the dependency on the separation side, i.e. emitter (front side) or emitter-free side (rear side). It is found that by conducting the LSMC process from the front side, a significantly lower energy conversion efficiency by $\Delta\eta = -1.9\%_{abs}$ in comparison to the rear side process is observed which originates in particular from a lower pseudo fill factor $\Delta pFF = -7.5\%_{abs}$. This is attributed to local ablation of the *p*-*n*-junction leading to increased j_{02}-like recombination. By conducting the laser scribe without subsequent mechanical cleaving of host cells, we measure $\Delta pFF = -9.1\%_{abs}$ in comparison to the initial host cell measurement. This indicates that the laser ablation process itself leads to the strong *pFF* and η losses observed after LSMC separation of *p*SPEER cells. In comparison, the TLS process is found to be invariant to the processed cell side. It is shown that in this case, the involved laser cleave process itself has no measurable impact on the performance of unseparated host cells.
Keywords: PERC, laser processing, thermal laser separation, TLS, laser scribe and mechanical cleave, LSMC

1 INTRODUCTION

The module integration of separated silicon solar cells such as half cells [1] or shingle cells [2] is an approach for an increase in module efficiency. Due to lower solar cell and string currents, the series resistance losses are reduced [3]. Laser scribe and mechanical cleaving (LSMC) — often referred to as "scribe and break" [4] — or thermal laser separation (TLS) [5] are examples for industrially relevant technologies for the separation of silicon wafers into half cells or shingle cells. Both involve two process steps as illustrated in Figure 1, where one step is considered the main laser process. Step 1 is a preparation step, leaving the host cell unseparated. The second step is the actual separation process. For LSMC the main laser process is the laser scribe (step 1), for TLS it is the laser cleave (step 2). For LSMC as well as TLS, it is crucial that both process steps are performed in the correct order. If one step is skipped, the host cell is left unseparated.

Previous studies have compared LSMC and TLS with respect to mechanical stability and electrical performance of separated cells [6, 7]. It has been shown that for a LSMC process conducted from the emitter-free side, the incurred damage can be assigned to the laser ablation process itself [8]. Additionally, it was found that LSMC conducted from the emitter side can lead to reduced parallel resistance for aluminum back surface field cells [9]. Considering TLS, we recently demonstrated that the laser cleave has no measurable impact on the passivation layers for passivated emitter and rear cells (PERC) if conducted from the rear side [10]. A comprehensive comparison between front and rear side separation of PERC cells, including LSMC and TLS processing, has not been demonstrated yet.

Since the separation step is performed as the last process step during cell fabrication, it additionally results in unpassivated edges which lead to a decreased energy conversion efficiency of shingle cells [11–15]. The efficiency loss of separated cells due to their unpassivated edge can be partly compensated by applying a postmetallization passivation layer [16].

In this paper, we analyze the impact of LSMC and TLS processing on the rear and front side of bifacial *p*-type silicon shingled passivated edge, emitter and rear (*p*SPEER) cells [17]. They feature a front side emitter as depicted in Figure 2. This means the processes are performed either on the side of the *p*-*n*-junction or on the opposite side. We divide our investigation into two experiments: In the first experiment, we analyze the impact of the main laser processes on unseparated host cells. This means (i) the laser scribe of the LSMC process is performed without mechanical cleaving and (ii) the laser cleave of the TLS is performed without applying the initial scribe. In both cases, the processed host cells are not separated and allow for a direct comparison of the current-voltage (IV) characteristics before and after the laser processes. In the second experiment, we perform the complete LSMC or TLS process from front or rear side to fabricate *p*SPEER cells which allows for the analysis of the complete separation process.

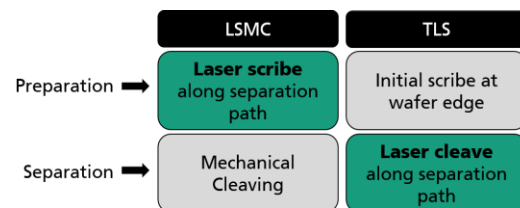

Figure 1: Overview of the two process steps involved in LSMC and TLS. The main laser processes for both are marked in green.

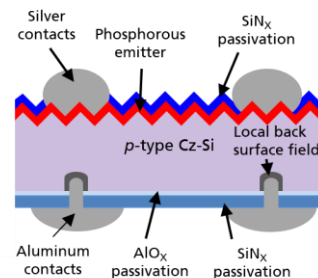

Figure 2: Schematic cross section of a bifacial PERC device. The *n*-type emitter is on the front side of the cell (SiN_X: silicon nitride, AlO_X: aluminum oxide, Cz-Si: Czochralski-grown silicon).

2 LASER SEPARATION TECHNOLOGIES

A manifold of technologies exist to separate brittle semiconductors such as silicon. Mechanical methods like diamond scratching and breaking, chip saw dicing [4] as well as a diversity of laser assisted processes, including stealth dicing [18], water-jet guided laser processing [19], laser direct cleaving [20], LSMC and TLS, are available. The laser-assisted methods have the advantage of contactless processing, reducing contamination and mechanical stress on the wafer. We present here in detail the LSMC and TLS process, both being industrially available and commonly used technologies for separation of solar cells in mass production. A variety of studies on those technologies and their impact on mechanical stability and electrical performance of solar cells has been published earlier [6, 8–10, 21].

The LSMC includes a laser ablation of silicon along the defined separation path (in the following referred to as laser scribe), followed by a mechanical cleaving step; see Figure **3**(a). The laser ablation depth reaches around one third of the sample thickness to allow for separation. A scanning electron microscope (SEM) image of a LSMC processed cell edge is shown in Figure 4(a).

For the TLS, depicted in Figure **3**(b), an initial short laser scribe at the wafer edge is applied. Subsequently, the cleaving process is conducted, including a continuous wave infrared (IR) laser that heats the material, followed by a water-air-aerosol cooling jet. The temperature difference (i.e. thermal gradient) results in compressive and tensile stresses, which lead to the cracking of the material along the guided path. The TLS process is a kerfless method resulting in optically smooth edges, since no damage of the crystal structure is induced. A SEM image of such an edge is shown in Figure 4(b).

In our experiments, the microDICE machine from 3D-Micromac AG is used for both, the LSMC and the TLS process. It includes a pulsed IR laser (wavelength $\lambda = 1070$ nm) for the scribe process (for both the LSMC laser scribe and the initial scribe for TLS) as well as the cleave unit consisting of a continuous wave IR laser ($\lambda = 1070$ nm) and a water-air nozzle [22].

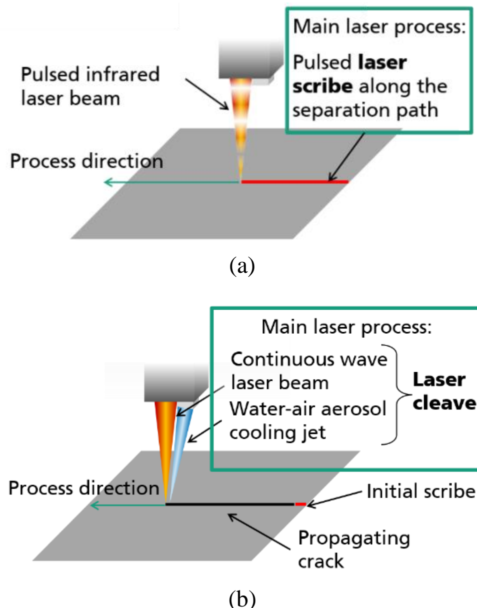

Figure 3: Schematic illustration of (a) the LSMC and (b) the TLS process.

3 EXPERIMENTS

The host cells are fabricated using industrial 6-inch boron-doped *p*-type Cz-Si PERC precursors. The cell fabrication process flow is shown in Figure **5**. After local laser contact opening on the rear side, the front and rear side metallization is applied by screen printing a firing through silver paste and an aluminum paste, respectively. The metallization layout is shown in Figure **6**. After a high temperature contact firing step, the cells undergo an ultrafast regeneration process [23] followed by light-induced degradation to obtain stable cell parameters.

The illuminated I-V characteristics such as fill factor or conversion efficiency are not meaningful in this case, since the metallization layout does not cover the whole cell area. Hence, initial SunsV_{OC} measurements of the host cells are conducted, contacting the fabricated host cells with a Gridtouch unit in an industrial cell tester at standard testing conditions [24]. From those measurements the pseudo fill facor (*pFF*) and open-circuit voltage V_{OC} can be obtained, to characterize edge recombination and laser damage to passivation layers. The initial SunsV_{OC} measurement serves two purposes. First, it allows for distributing the host cells into two groups with four subgroups each, making sure that similar *pFFs* are present among the subgroups. Secondly, it is the reference measurement for the first experimental group.

The two main groups are assigned to two different experimental approaches. The experimental process flow is shown in Figure **7**. In the first host cell group, we analyze the sole influence of the two main laser processes (laser scribe and laser cleave) on the solar cells' *pFF* and V_{OC} without separating the host cells. In the second group, *p*SPEER cells are cut out of the host cells to analyze the separated cell performance, including both, the effect of the main laser process as well as of complete separation.

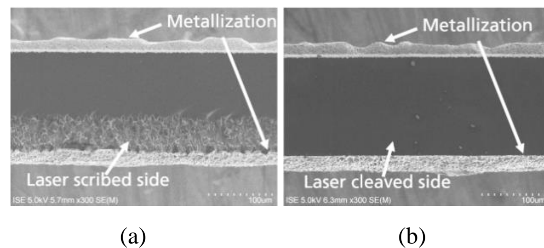

(a) (b)

Figure 4: SEM images of (a) a LSMC and (b) a TLS separated cell edge.

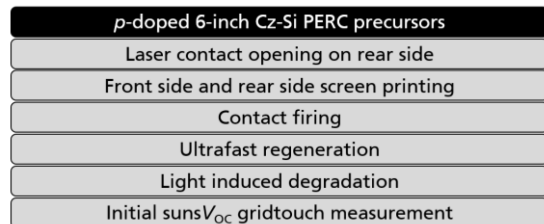

Figure 5: Process flow for the fabrication of the *p*SPEER host cells. With an initial SunsV_{OC} measurement, the cells are sorted into groups with similar *pFF*s.

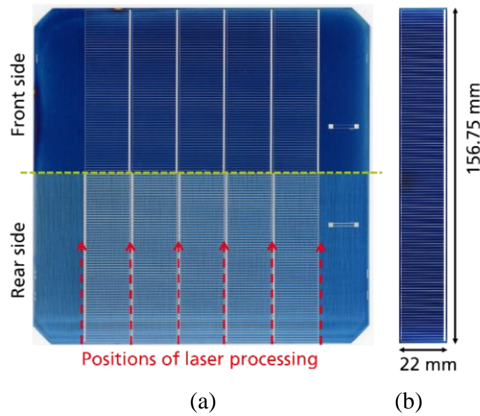

(a) (b)

Figure 6: (a) Merged images of the metallization layouts of the host cells' front side (top) and rear side (bottom) including five *p*SPEER cells with the dimension 22 mm x 156.75 mm. The dotted lines indicate the laser processing paths. (b) Image of the front side of a separated *p*SPEER cell. The layout was designed for research purposes not covering the whole wafer area, which is not industrially beneficial.

3.1 Analysis of the main laser processes

The influence of the main laser processes (group 1 in Figure **7**) on *pFF* and V_{OC} of host cells is analyzed by not performing the complete separation but just the main laser process involved in the two separation technologies. In the case of LSMC, only the laser scribe is performed without mechanically cleaving the cells. For the TLS process, the cleave step is performed without applying the initial scribe. Hence, the host cells in group 1 remain in the full wafer-sized format after the laser processes. These processes are performed either from the front side (FS) or the rear side (RS) of the host cells, resulting in four subgroups. After laser processing, the cells undergo a light-induced degradation step to eliminate any laser process effect on the boron-oxygen defect state. The effect of the laser processes is characterized by comparing SunsV_{OC} measurements after the laser processing to the initial SunsV_{OC} measurements, which are done after host cell fabrication as described earlier.

3.2 Analysis of complete laser-assisted separation

The host cells of group 2 are separated by the full LSMC and TLS processes to obtain *p*SPEER cells. Both processes are performed from the host cell front side or rear side resulting in four subgroups. As described earlier an additional light-induced degradation step after laser processing is conducted. To characterize the effect of the laser separation processes, IV measurements are performed after the separation. The measurement is conducted in a cell tester by contacting the cell busbars with pin arrays. During the measurement, the cells are placed on a black, non-conducting chuck to ensure a monofacial measurement without additional contribution of the rear side. It is not reasonable to compare these IV measurements to any initial measurements due to the metallization layout. Additionally, the electrical contacting for the host cells is just possible by a Gridtouch unit while the *p*SPEER cells can only be contacted by pins. Hence, also the initial SunsV_{OC} measurements are not comparable to the *p*SPEER results. Merely, the IV measurements obtained from the different groups are compared among each other to determine differences between the processes.

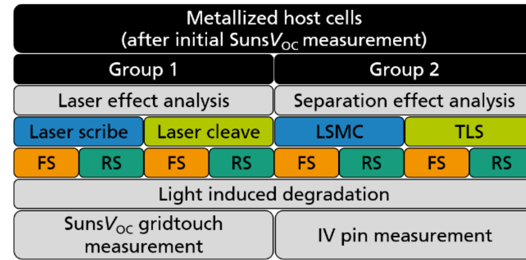

Figure 7: Process flow for the experimental investigation of the LSMC and TLS process influence on cell performance. Group 1 investigates the main laser process influence. In group 2 the fully separated *p*SPEER cells are analyzed which includes the effect of recombination at the edge after complete separation.

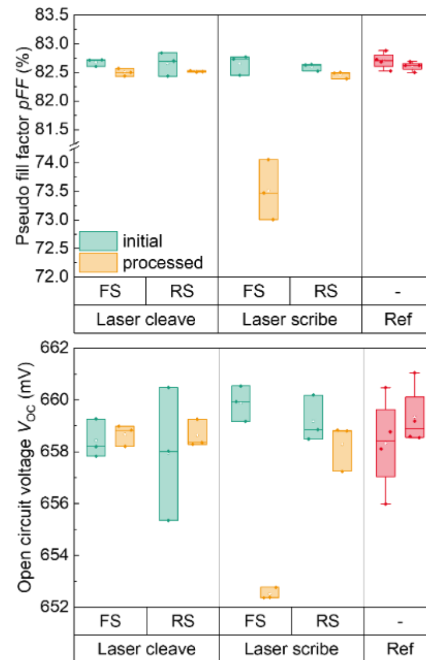

Figure 8: SunsV_{OC} results of the host cells before and after the main laser processes "laser scribe" and "laser cleave". An unprocessed reference group Ref is also presented (in red) to check for a stable measurement.

4 RESULTS AND DISCUSSION

The mean V_{OC} and *pFF* of the fabricated host cells are measured by the initial SunsV_{OC} measurements to be $V_{OC} = (659 \pm 1)$ mV and $pFF = (82.7 \pm 0.2)\%$. The cells are allocated in two main groups with similar mean *pFF*, which results in slight differences in V_{OC} among the groups of 2 mV. These measurements serve as reference for the analysis of the laser effect on unseparated host cells.

4.1 Effect of the main laser processes on host cells

The V_{OC} and *pFF* resulting from the SunsV_{OC} measurements of the unseparated host cells before and after the laser scribe or laser cleave processing are shown in Figure **8**. A reference group is shown which is measured without being processed, exhibiting a slightly increased V_{OC} by $\Delta V_{OC} = 2$ mV and a lower *pFF* by $\Delta pFF = -0.1\%_{abs}$ in the second measurement. Considering this, both laser cleaved cell groups show no change in V_{OC} or *pFF*, independent of the processing side. For the rear side laser

scribed cells, a $\Delta V_{OC} = -1$ mV is measured while no measurable change in pFF occurs. The front side laser scribed cells, however, show a strong decrease of $\Delta V_{OC} = -7$ mV and $\Delta pFF = -9.1\%_{abs}$.

The measurements show the sole influence of the main laser processes on the whole cell structure. For the laser cleave, the passivation layers and silicon wafer are not degraded during the process, independent of the processing side. The laser scribed samples, however, show a clear difference between front and rear side processing. Since the laser ablates up to one third of the cell thickness, the scribe itself is already damaging the silicon and passivation layers. This effect becomes severe once the process is conducted from the front side. Then, the laser process ablates the *p*-*n*-junction leading to increased recombination as it can be deduced from the strong V_{OC} and pFF decrease.

4.2 Effect of the complete separation processes

The IV measurement results of separated *p*SPEER cells are shown in Figure **9** comparing the LSMC and TLS processes conducted from front side and rear side on the host cells. Independently of the process and process side, the designated short-circuit current density $j_{SC,des}$ (excluding the busbar area [11]) is measured to be $j_{SC,des} = 40.6$ mA/cm^2 at a constant series resistance $R_S = 0.4$ Ωcm^2. Both TLS separated groups as well as the LSMC RS group show similar efficiencies $20.5\% < \eta < 20.7\%$, featuring $81.4\% < pFF < 81.9\%$ and $657 \text{ mV} < V_{OC} < 659$ mV. In comparison, a significantly low $\eta = 18.5\%$ is measured for the LSMC FS group, which results from $pFF = 73.9\%$ as well as $V_{OC} = 654$ mV. Although the parallel resistance $R_P = 9$ kΩcm^2 is quite small, it is still high enough to not have an effect on pFF. The lower pFF by $\Delta pFF = -7.5\%_{abs}$ of the LSMC FS group in comparison to the LSMC RS group is assigned to increased j_{02}-like recombination at the *p*-*n*-junction, as discussed earlier. Comparing the main laser process influence from the previous chapter to the complete separation process shows, that most of the pFF loss resulting from *p*SPEER cell separation is caused by the laser scribe process itself. Hence, the major contribution is the ablation through the *p*-*n*-junction. The full separation, namely the mechanical breaking of the remaining cell thickness (i.e. non-ablated edges), and additionally arising open edge does not contribute significantly to the comparably low pFF and η of the LSMC FS group.

As it is found in the first experiment for the laser cleave, the processed cell side does not have an influence on the pFF and V_{OC} of host cells. This observation holds for the full TLS process as well. Since the cleave laser is an IR laser, absorption occurs within the whole substrate thickness, due to the low absorption coefficient of silicon in the IR range. Therefore, the material is heated uniformly throughout the whole cell thickness and the processed cell side is not relevant for either the laser cleave nor the full TLS process.

Although slight differences are measured between the two TLS groups and the LSMC RS group, it is difficult to draw definite conclusions since the measurements cannot be compared to any initial IV cell measurements. Therefore, we do not consider those differences being significant in our experiment. For a more elaborated investigation, the host cell layout can be designed such to lead to meaningful IV measurements by covering the whole precursor area. Additionally, it should be measurable by the same contacting unit as the *p*SPEER cells to allow for an accurate comparison before and after laser processing. The found advantage of the TLS process lies in its invariance to the processed cell side. Furthermore, it has been demonstrated that edges obtained by TLS can be successfully passivated by an additional postmetallization edge passivation to compensate edge recombination losses [16].

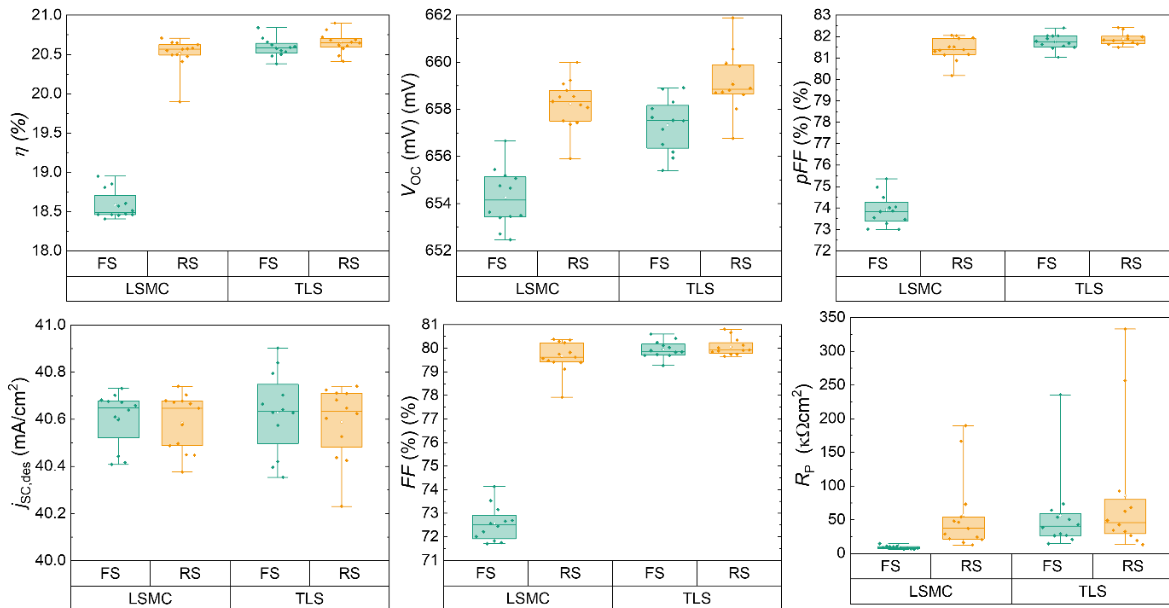

Figure 9: Designated area IV measurement results for FS and RS separated *p*SPEER cells by LSMC and TLS. By excluding the busbar area which would be covered during a shingled cell module integration, the designated area short-circuit current density $j_{SC,des}$ is given.

5 SUMMARY AND CONCLUSION

This study compares the two laser assisted separation technologies laser scribe and mechanical cleaving (LSMC) and thermal laser separation (TLS). Both technologies comprise of two process steps, of which one is considered the main laser process, conducted along the whole separation path. The influence of the two separation technologies and their main laser processes on the electrical performance of separated *p*-type shingled passivated edge, emitter and rear (*p*SPEER) cells is investigated. These cells feature a front side emitter. In our investigation we include an analysis of the influence of the processed cell side (i.e. emitter and emitter-free side).

It is found that the LSMC process, conducted from the cells' front side, leads to a comparably low $\eta = 18.6\%$ ($\Delta\eta = 1.9\%_{abs}$ in comparison to the LSMC rear side separated group). This results from a lower pseudo fill factor *pFF* by $\Delta pFF = -7.5\%_{abs}$. The low *pFF* indicates a local destruction of the *p*-*n*-junction by the ablating laser process and hence increased j_{02}-like recombination. This result is confirmed by the study of the sole laser process involved in LSMC, namely the laser scribe. A significant *pFF* loss is observed after performing the laser scribe on the front side of host cells, leaving them unseparated. Hence, the low *p*SPEER cell performance of LSMC front side separated cells originates from the laser scribe process itself.

However, *p*SPEER cells separated by LSMC from the rear side show a comparable performance to TLS separated cells. For TLS, the processed cell side shows no influence on the cell performance. An investigation of the laser cleave, being the main laser process for TLS, shows that no measureable effect on *pFF* or V_{OC} is observed for processed, unseparated host cells.

Therefore, we emphasize on the importance of the chosen process side, depending on the position of the emitter, if a LSMC process is conducted. The TLS process shows the advantage of being invariant to the cell side on which the process is performed, which makes it the more flexible laser assisted separation process.

ACKNOWLEDGEMENTS

The authors would like to thank the colleagues at Fraunhofer ISE PV-TEC; especially M. Retzlaff, D. Witt, T. Nguyen and R. Eberle. This work was funded by the German Federal Ministry for Economic Affairs and Energy within the research project "PV-BAT400" (contract number 0324145).

REFERENCES

[1] J. Schneider, S. Schoenfelder, and S. Dietrich, et al. "Solar Module with Half Size Solar Cells" in *29th European Photovoltaic Solar Energy Conference and Exhibition*, Amsterdam, The Netherlands, 2014, pp. 185–189, doi:10.4229/EUPVSEC20142014-1BV.6.48.

[2] J. D. C. Dickson, "Photo-voltaic semiconductor apparatus or the like," US2938938A, May 31, 1960.

[3] S. Guo, J. P. Singh, and I. M. Peters, et al. "A Quantitative Analysis of Photovoltaic Modules Using Halved Cells", *International Journal of Photoenergy*, pp. 1–8, 2013, doi:10.1155/2013/739374.

[4] W.-S. Lei, A. Kumar, and R. Yalamanchili "Die singulation technologies for advanced packaging: A critical review", *Journal of Vacuum Science & Technology B, Nanotechnology and Microelectronics: Materials, Processing, Measurement, and Phenomena*, vol. 30, no. 4, p. 40801, 2012, doi:10.1116/1.3700230.

[5] H.-U. Zuhlke, G. Eberhardt, and R. Ullmann "TLS-Dicing - An innovative alternative to known technologies" in *IEEE/SEMI Advanced Semiconductor Manufacturing Conference*, Berlin, Germany, 2009, pp. 28–32, doi:10.1109/ASMC.2009.5155947.

[6] F. Kaule, M. Pander, and M. Turek, et al. "Mechanical damage of half-cell cutting technologies in solar cells and module laminates" in Lausanne, Switzerland, 2018, p. 20013, doi:10.1063/1.5049252.

[7] S. Eiternick, F. Kaule, and H.-U. Zühlke, et al. "High Quality Half-cell Processing Using Thermal Laser Separation", *Energy Procedia*, vol. 77, pp. 340–345, 2015, doi:10.1016/j.egypro.2015.07.048.

[8] S. Eiternick, K. Kaufmann, and J. Schneider, et al. "Loss Analysis for Laser Separated Solar Cells", *Energy Procedia*, vol. 55, pp. 326–330, 2014, doi:10.1016/j.egypro.2014.08.094.

[9] M. Oswald "Evaluation of Silicon Solar Cell Separation Techniques for Advanced Module Concepts" in *28th EU PVSEC 2013*, pp. 1807–1812.

[10] P. Baliozian, A. Münzer, A. Nair, E. Lohmüller, T. Fellmeth, N. Wöhrle, H. Höffler, A. Spribille, R. Preu "Thermal laser separation of PERC and SHJ solar cells", *IEEE J. Photovoltaics*, 2020, (submitted).

[11] N. Wöhrle, T. Fellmeth, and E. Lohmüller, et al. "The SPEER solar cell – simulation study of shingled PERC technology based stripe cells" in *33rd European Photovoltaic Solar Energy Conference and Exhibition*, Amsterdam, The Netherlands, 2017, doi:10.4229/EUPVSEC20172017-2CV.2.33.

[12] Hermle, M., Dicker, J., Warta, W., Glunz, S. W., & Willeke, G "Analysis of edge recombination for high-efficiency solar cells at low illumination densities" in *3rd World Conference on Photovoltaic Energy Conversion*, Osaka, Japan, 2003.

[13] N. Wöhrle, E. Lohmüller, and M. Mittag, et al. "Solar cell demand for bifacial and singulated-cell module architectures", *Photovoltaics International*, vol. 36, pp. 48–62, 2017.

[14] P. Baliozian, N. Klasen, and N. Wöhrle, et al. "PERC-based shingled solar cells and modules at Fraunhofer ISE", *Photovoltaics International*, no. 43, 129-145, 2019.

[15] K. R. McIntosh "Lumps, humps and bumps: Three detrimental effects in the Current-Voltage curve of Silicon solar cells" Dissertation, Centre for Photovoltaic Engineering, University of New South Wales, Sydney, 2001.

[16] P. Baliozian, M. Al-Akash, and E. Lohmuller, et al. "Postmetallization "Passivated Edge Technology" for Separated Silicon Solar Cells", *IEEE J. Photovoltaics*, vol. 10, no. 2, pp. 390–397, 2020, doi:10.1109/JPHOTOV.2019.2959946.

[17] P. Baliozian, E. Lohmüller, and T. Fellmeth, et al. "Bifacial p-Type Silicon Shingle Solar Cells − the

"pSPEER" Concept", *Sol. RRL*, vol. 2, no. 3, p. 1700171, 2018, doi:10.1002/solr.201700171.

[18] M. Kumagai, N. Uchiyama, and E. Ohmura, et al. "Advanced Dicing Technology for Semiconductor Wafer—Stealth Dicing", *IEEE Trans. Semicond. Manufact.*, vol. 20, no. 3, pp. 259–265, 2007, doi:10.1109/TSM.2007.901849.

[19] B. Richerzhagen, M. Kutsuna, and H. Okada, et al. "Waterjet-guided laser processing" in *Third International Symposium on Laser Precision Microfabrication*, Osaka, Japan, 2002, p. 91, doi:10.1117/12.486514.

[20] INNOLAS solutions, *INNOLAS SOLUTIONS - LASER FOR CLEAVING.* [Online] Available: https://www.innolas-solutions.de/medien/news-pr/details/innolas-solutions-laser-for-cleaving/. Accessed on: Jul. 15 2020.

[21] D. Lewke, *Untersuchung und Minimierung lateraler Rissabweichungen beim Thermischen Laserstrahlreparieren*. Aachen: Shaker Verlag, 2018.

[22] 3D-Micromac AG, *TLS-Dicing™ System for Separation of Silicon and Silicon Carbide Wafers.* [Online] Available: https://3d-micromac.com/laser-micromachining/products/microdice/. Accessed on: Jul. 02 2020.

[23] A. A. Brand, K. Krauß, and P. Wild, et al. "Ultrafast In-Line Capable Regeneration Process for Preventing Light Induced Degradation of Boron-Doped p-Type Cz-Silicon Perc Solar Cells" in *33rd EU PVSEC*, Amsterdam, The Netherlands, 2017, pp. 382–387, doi:10.4229/EUPVSEC20172017-2CO.9.5.

[24] N. Bassi, C. Clerc, and Y. Pelet, et al. "GridTOUCH: Innovative Solution for Accurate IV Measurement of Busbarless Cells in Production and Laboratory Environments" (eng), 2014, doi:10.4229/EUPVSEC20142014-2BV.8.24.